Toxicol Res. (2023) 39:213–229
https://doi.org/10.1007/s43188-022-00158-w

Online ISSN 2234-2753
Print ISSN 1976-8257

ORIGINAL ARTICLE

Assessment of toxicity and genotoxic safety profile of novel fisetin ruthenium-p-cymene complex in mice

Ishita Seal[1] · Sidhanta Sil[1] · Abhijit Das[1] · Souvik Roy[1]

Received: 23 July 2022 / Revised: 15 November 2022 / Accepted: 22 November 2022 / Published online: 12 December 2022

Abstract

Throughout the last decades flavonoids have been considered as a powerful bioactive molecule. Complexation of these flavonoids with metal ions demonstrated the genesis of unique organometallic complexes which provide improved pharmacological and therapeutic activities. In this research, the fisetin ruthenium-p-cymene complex was synthesized and characterized via different analytical methods like UV–visible spectroscopy, Fourier-transform infrared spectroscopy, mass spectroscopy, and scanning electron microscope. The toxicological profile of the complex was evaluated by acute and sub-acute toxicity. Additionally, the mutagenic and genotoxic activity of the complex was assessed by Ames test, chromosomal aberration test, and micronucleus based assay in Swiss albino mice. The acute oral toxicity study exhibited the LD_{50} of the complex at 500 mg/kg and subsequently, the sub-acute doses were selected. In sub-acute toxicity study, the hematology and serum biochemistry of the 400 mg/kg group showed upregulated white blood cells, aspartate aminotransferase, alanine aminotransferase, alkaline phosphatase, creatinine, glucose and cholesterol. However, there was no treatment related alteration of hematological and serum biochemical parameters in the 50, 100, and 200 mg/kg group. In the histopathological analysis, the 50, 100, and 200 mg/kg groups were not associated with any toxicological alterations, whereas the 400 mg/kg group showed prominent toxicological incidences. Nevertheless, the treatment with fisetin ruthenium-p-cymene complex did not exhibit any mutagenic and genotoxic effect in Swiss albino mice. Thus, the safe dose of this novel organometallic complex was determined as 50, 100, and 200 mg/kg without any toxicological and genotoxic potential.

Keywords Fisetin · Ruthenium-p-cymene · Organometallic complex · Flavonoids · Toxicity study

Introduction

Flavonoids are naturally occurring polyphenolic phytochemicals found in a wide range of plants which involved in a number of biological processes [1]. Flavonoids are group of secondary metabolites consist of polyphenolic structure, more specifically phenyl benzo-γ-pyrones derivatives [2]. Their ring structure comprises a basic C_6-C_3-C_6 skeleton which consist of two aromatic rings (A ring and B ring) linked by a heterocyclic pyran and pyron ring (C ring) and connected by three carbon atoms (Fig. 1A). The flavonoids can be classified into six groups based on their chemical structure which include flavonols, flavanonols, flavonones, flavones, isoflavones, and anthocyanins [3]. In the current age, the flavonoids have demonstrated a wide variety of pharmacological advancements, including antioxidant, anticancer, anti-cardiocerebrovascular disease and anti-inflammatory activities [4–6]. Thus, fisetin, a flavonol moiety, has piqued the interest of many researchers due to its diverse pharmacological properties.

Fisetin (3, 7, 3′, 4′ – tetrahydroxyflavone) is the most ubiquitous bioactive flavonol, commonly found in the smoke tree *(Cotinus coggygria)* and in various fruits and vegetables like strawberries, apples, persimmons, kiwis, onion, tomatoes and cucumber [7]. Additionally, fisetin can also be found in the majority of human diets, especially those derived from plants. Fisetin exerts a wide variety of biological effects like antineoplastic, cardioprotective, neuroprotective, antidiabetic, antiviral, anti-inflammatory and anti-allergic activities [8, 9] and also endeavor multi-targeted neuro-protective effects by reducing oxidative stress, neuroinflammation, apoptotic cell death and synaptic dysfunction

✉ Souvik Roy
souvikroy35@gmail.com; souvik.roy@nshm.com

[1] Department of Pharmacy, NSHM Knowledge Campus Kolkata-Group of Institution, 124 B.L. Saha Road, Tara Park, Behala 700053, West Bengal, India

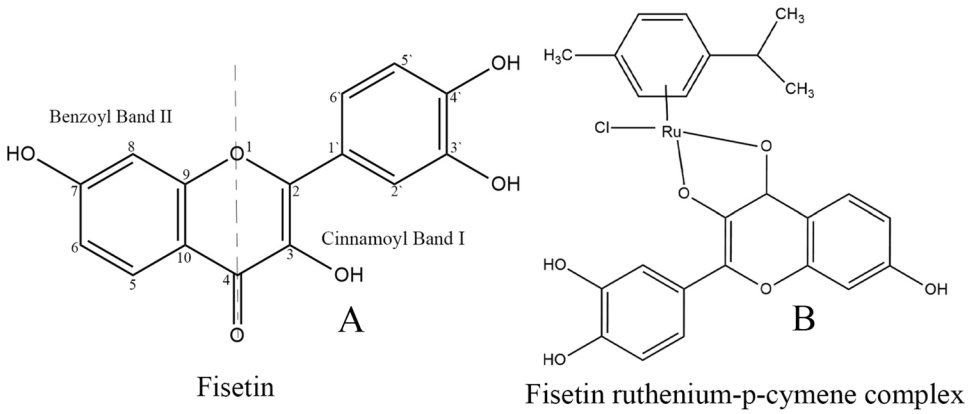

Fig. 1 Basic structure of **A** fisetin and **B** fisetin ruthenium-p-cymene complex

in the brain [10]. Fisetin reduced histological damage, malondialdehyde levels, inflammasome pathway activation, apoptosis, improved BDNF expression, decreased astrocyte, microglial activation, and cognitive impairments. Fisetin exerts these protective activities through the suppression of ROS-induced NF-κB/NLRP3 inflammasome activation and increased expression of antioxidant Nrf2/HO-1 [11]. In mouse macrophages, induction of LPS generated an inflammatory response that prevented autophagosome-lysosome fusion and degradation in which administration of fisetin caused blocking of PI3K/AKT/mTOR signalling pathway. In addition, fisetin also reduced the production and secretion of inflammatory cytokines and promoted autophagosome-lysosome fusion and destruction in LPS-treated RAW264.7 cells [12]. Furthermore, a strong antioxidant activity has also been reported for fisetin which diminish the effects of free radicals generation by the presence of hydroxyl groups. Fisetin has also exerted excellent metal chelating properties [13] by which it can form metal complexes. The properties of the organometallic complex can be influenced by the number, position of the substituents and type of metal ion [14–16]. Studies have demonstrated that fisetin have complex formation ability with various metal ions like Al(III), Cu(II), Zn(II) and Pb(II) at ligand chelation sites (3-hydroxy-4- Oxo and 3´,4´-dihydroxy group) (Fig. 1B) [17]. It was suggested that the biological activity of flavonoid were increased when coordinated with metal ion due to its free radical accepting property [18, 19]. Moreover, an increase in antioxidant properties of flavonoids has been noted after metal complexation [20].

Metal complexes have played an essential part in therapy for about 5000 years due to their physico-chemical characteristics, variable oxidation states, hydrophobicity and lipophilicity, high aqueous solubility and positively charged nature [21–23]. In this instance, cisplatin, a platinum (II) containing anticancer drug was often used to treat a wide range of cancers [24, 25]. However, severe side effects such as myelotoxicity, peripheral neuropathy were reported for platinum-based anticancer drugs [26, 27]. In order to overcome the current adversities, researchers have developed a keen interest in the exploration of new metal ions with lesser side effects and greater pharmacological efficacy. On this occasion, ruthenium complex show several benefits over platinum metals such as several oxidation states, ligand exchange kinetics, and iron mimicking properties. Moreover the attachment of a hydrophobic moiety, n^6-p-cymene, leads to increased cellular accumulation and better biodistribution of ruthenium-metal complex through passive diffusion [28].

Based on the above findings, in this study, a novel organometallic complex, fisetin ruthenium-p-cymene-complex has been synthesized, characterized and toxicological profile was assessed via evaluating the genotoxic potential of the complex. It is the first time where the organometallic complex of fisetin has been synthesized and the LD_{50} value of this novel complex was determined via toxicity study. In addition, the NOAEL doses was discovered through subacute toxicity study which can be further used for various pharmacological and therapeutic intervention.

Materials and methods

Chemicals and materials

Fisetin (3, 7, 3′, 4′ – tetrahydroxyflavone), and dichloro ruthenium-p-cymene dimer, cyclophosphamide, colchicine, histidin, biotin, and bovine serum albumin were purchased from Sigma Aldrich (St. Louis, MO, USA). 2, 4, 7-trinitro-9-fluorenone was procured from TCI Chemicals Pvt. Ltd. Extra pure methanol, DPPH (2, 2 -Diphenyl-2-Picrylhydrazyl), ABTS (2, 2'-azinobis (3-ethylbenzothiazoline-6-Sulphonic acid diammonium salt)), TPTZ (2, 4, 6-Tripyridyl-S-triazine) were purchased from Sigma Aldrich Chemical Co (St. Louis, MO, USA). All the reagents were procured from local store at highest purity level.

Synthesis of fisetin-ruthenium-p-cymene complex

The fisetin ruthenium-p-cymene complex was synthesized by incorporating both fisetin and ruthenium-p-cymene moiety in a 2:1 ratio at a specific reaction condition. Approximately 28.6 mg (0.1 mmol) of fisetin was weighed and dissolved in ethanol in dark condition for 1 h and maintain the pH at 6. Approximately 30.62 mg (0.05 mmol) of ruthenium-p-cymene was dissolved in dichloromethane and the solution was continuously added the fisetin solution in dark condition for 24 h. Then the solvent in the beaker was evaporated in room temperature and the greenish black color precipitate was collected (Fig. 1B).

Physical measurements of the complex

UV–visible spectroscopical data of fisetin and fisetin ruthenium-p-cymene complex were analyzed by UV-1900i Shimadzu double beam spectrophotometer. Fourier-transform infrared spectroscopy (FT-IR) spectrum of fisetin and the complex were evaluated by FT-IR (IRAffinity-1S, Shimadzu) over the range of 500–4000 cm^{-1} wave number to determine the metal oxide bond as a validation of the complexation. The structural elucidation of the complex was done using ESI-MASS spectroscopy (XEVO G2 Xs Q-Tof ESI Mass). The surface morphology of the complex was determined by the scanning electron microscopy (SEM) technique (JEOL MAKE, (UK) Model-JSM-IT800 Schottky Field Emission Scanning Electron Microscope) at an accelerating voltage of 5 kV, and the complex was examined at different magnification (4000X, 4500X, 6000X and 10,000X).

Assessment of antioxidant activity status of fisetin ruthenium-p-cymene complex

DPPH (1,1-diphenyl-2-picrylhydrazyl), ferric reducing antioxidant power (FRAP), ABTS (2,2′-azino-bis-3-ethylbenzthiazoline-6-sulphonic acid) methods were used to determine the antioxidant activity of fisetin and fisetin ruthenium-p-cymene complex.

Assessment of antioxidant status of the complex using DPPH method

According to the Rahman and his co-researchers, the antioxidant activity of the complex was measured by the DPPH free radical scavenging assay method [29]. 0.1 mM DPPH was dissolved in ethanol and this solution was added to the solution of the complex at different concentrations (12.5, 25, 50, 75, 100, 125, and 150 µg/mL). At 517 nm, the mixture absorbance was determined. This equation was used to calculate the % DPPH radical scavenging activity:

$$\%\ \text{DPPH radical scavenging activity} = \{(A0 - A1)/A0\} \times 100\%$$

where A0 is the absorbance of the control, and A1 is the absorbance of the compound at different concentrations. % of inhibition was plotted against concentration.

Assessment of antioxidant status of the complex using FRAP method

The antioxidant activity of the complex was also analysed using FRAP method according to the protocol described by Benzie and Strain (Benzie and Strain 1996) which was advanced by Griffin and Bhagooli [31]. The antioxidant potential was measured by the ability of the complex to reduce Fe^{3+} ion. In this assay, the TPTZ solution and $FeCl_3$ were combined in newly made acetate buffer to prepare the FRAP reagent. The bluish color of the Fe^{3+} ion in TPTZ solution changes its color to dark as it reacts with the antioxidant substance and reduced to Fe^{2+} ion. The experiment was conduct by using different concentration of the fisetin ruthenium-p-cymene complex as well as by busing free fisetin. The absorbance of the solution was measured at 593 nm.

Assessment of antioxidant status of the complex using ABTS method

According to Pennycooke, COX & Stushnoff was used to measure the antioxidant efficacy of the complex by ABTS method with little modification [32]. 1 gm of MnO_2 was added after 54.2 mg of ABTS powder had been mixed in 10 ml of phosphate buffer solution (5 mM and pH 7.0). Greenish-colored solution was observed after 30 min of room temperature incubation. Centrifugation was performed for 5–6 min at 4 °C and 10,000 rpm, then the solution was incubated for around 30 min at room temperature and identified the greenish color solution. The filtrate was diluted with phosphate buffer after filtration until the final solution absorbance was equal to 0.70 ± 0.01 at 723 nm. In 2 ml of ABTS solution, different concentration (2 µm to 15 µm) of fisetin and fisetin ruthenium-p-cymene complex were added, and then it is incubated for 10 min at room temperature. After 10–12 min, by using UV–Visible spectroscopy at 734 nm decrease in ABTS absorbance was observed. The % ABTS radical scavenging activity was calculated by this equation:

$$\text{Radical Scavenging activity at 734 nm (\%)} = 1 - \text{Af}/\text{A0} * 100$$

where, A0 = Absorbance of uninhibited radical cation, Af = Absorbance measured 10-min after addition of the complex.

Animal

Swiss Albino mice (20–30 g) of both sex were acquired from a registered animal breeder (1828/PO/Bt/S/15/CPCSEA dated 14.09.2015). Animals were placed in plastic cages and 12 h light /12 h dark cycle was maintained at 22 ± 3 °C, relative humidity of 52–57%. The animals were given food and water ad libitum. The animal experiment was approved by the Institutional Animal Ethics Committee and by the Animal Regulatory Body of the Government (Regd. No. 1458/PO/E/S/11/CPCSEA dated 12.05.2011) and the IAEC protocol number (NCPT/IAEC/007/2022).

Acute toxicity study

The acute oral toxicity study of the fisetin ruthenium-p-cymene complex was carried out according to the OECD Guideline TG-420 (adopted in December 2001) for the evaluation of the LD_{50} dose of the complex. The animals were fasted overnight prior to the toxicity study. Sixteen Swiss Albino mice**,** 8 of each sex (females should be nulliparous and nonpregnant), were distributed into four groups (four animals per group and two of each sex). The animals were allocated as: Group I- normal control (supplied with carboxymethyl cellulose (CMC) 0.5%). Group II- 500 mg/kg complex. Group III- 1000 mg/kg complex. Group IV- 2000 mg/kg complex. After the administration of the organometallic complex animals were monitored for mortality for up to three days.

Sub-acute toxicity study

According to the OECD Guideline TG-407 (adopted in December 2001), the sub-acute toxicity study was conducted. The animals were fasted overnight prior to the toxicity study. Thirty Swiss Albino mice**,** 15 of each sex were randomly divided into five groups (six animals per group and three of each sex). The animals were distributed as Group I- normal control (carboxymethyl cellulose (CMC) 0.5%). Group II- 50 mg/kg complex. Group III- 100 mg/kg complex. Group IV- 200 mg/kg complex. Group V- 400 mg/kg complex. The animals were supplemented with adequate food and water instantly prior to the treatment with the complex. The animals were monitored for general clinical appearance, body weights, and mortality for up to 28 days. Animals were euthanized under the anesthesia of pentobarbital sodium (45 mg/kg, i.p) and investigated for hematological, serum biochemical, and histopathological evaluations.

Body weight and water consumption

The body weights of each animal were recorded at weekly intervals. The water consumption of each animal (ml/animal/day) was also measured on a weekly basis.

Hematology and serum biochemistry

The blood samples were collected from the retro-orbital plexus of mice which were then analyzed immediately. The hematological parameters were investigated by Medonic CA-20 cell analyzer systems (Boule Medical, Stockholm, Sweden). The serum was collected by centrifugation at 3500 rpm for 15 min and then analyzed by Microlab 3000 auto-analyzer to determine serum biochemical parameters including alanine aminotransferase (ALT), aspartate aminotransferase (AST), alkaline phosphatase (ALP), glucose, creatinine, and blood urea nitrogen (BUN).

Organ weight analysis

The animals were euthanized and the macroscopic abnormalities were carefully observed upon the completion of the study period. The weights of key organs like the liver, pancreas, kidney, testis, stomach, and ovary were assessed in both absolute and relative terms (organ to body weight ratio).

Histopathology

After sub-acute toxicity study, all the mice were sacrificed and vital organs (liver, pancreas, kidney, testis, stomach and ovary) were excised and fixed for 24 h in formalin. The excised organs were dehydrated and embedded in paraffin wax. The tissues of 5 µm thickness were kept on glass slides and rehydrated by graded alcohol. The slides were stained using hematoxylin and eosin (H&E), which were observed under the light microscope (Labline Olympus Microscope LED, MX21i) for histological evaluation [10X, 40X] and the images were evaluated by LCmicro 2.1 (Build 15,717).

Genotoxicity studies

Mutagenicity by Ames test

The Ames test for mutagenicity testing of the complex was carried out according to the method described by Maron and Ames. The mutagenic potential of the complex at various doses (5, 10, 20, and 40 mg/plate) was determined in the TA98 strain of *Salmonella typhimurium* with or without S9-mediated metabolism of the culture media. A particular colony of Salmonella strain was inoculated from the culture media to the master plate and kept overnight at 37 °C with

continuous stirring at 120 rpm. The bacterial culture was then treated with 5, 10, 20, and 40 mg/plate of the complex and added to histidine and biotin supplemented melted agar. The suspension of the test strain was further treated with S9 (5% v/v) rat liver extract, transferred to glucose minimal plates, and incubated for two days at 37 °C. The revertant colonies of the different complex treated groups were counted manually. In addition, the vehicle control (100 µl culture/plate DMSO) and the positive control were also utilized. In this regard, 2,4,7-trinitro-9-fluorenone and 2-aminofluorene were used as a positive control in the presence and absence of S9 liver extract [33].

Chromosomal aberrations test

The in vitro chromosomal aberration test was conducted in accordance with OECD guideline TG-473. The animals weighing 22 ± 5 g were distributed into six groups (Group I, II, III, IV, V, and VI) (6 animals each). Group I was assigned as the control group which received CMC in distilled water. Cyclophosphamide (CPA) (40 mg/kg i.p.) was administered to Group II animals at intervals of 24 h throughout the course of two days. The animals of Group III, IV, V, and VI were treated with 4 different doses of fisetin ruthenium-p-cymene complex (50, 100, 200, and 400 mg/kg). 0.05% colchicine was given intraperitoneally to the animals before euthanization for metaphase arrest. The bone marrow was extracted from the femur bone and suspended in 0.075 M potassium chloride solution. The supernatant was collected after centrifugation of bone marrow suspension at 4000 rpm. The obtained pellet was fixed by methanol:acetic acid (3:1) solution and further centrifuged at 3000 rpm for 10 min. The slides were dried and dyed for 15 min with 1 × Giemsa. An oil immersion optical microscope was used to screen the smears in 1000 × magnification, and images were analyzed using Axiovision Release 4.2 (06-2004) software.

Bone marrow micronucleus assay

According to OECD guidelines (TG-474), the in vivo bone marrow micronucleus assay was performed and similar experimental groups and doses were followed as chromosome aberration test. The bone marrow was extracted in 5% fetal bovine serum from the femur bone and centrifuged at 4000 rpm for 15 min. On glass slides that had been chemically cleaned, the smears from the pellet were prepared and stained using 1 × Giemsa stain. The polychromatic erythrocytes (PCEs) and normochromatic erythrocytes (NCEs) were stained reddish-blue and orange respectively, whereas the nuclear materials were visualized as dark purple stain. An oil immersion optical microscope was used to screen and analyze the smears in 1000X magnification. The proportion of polychromatic erythrocytes to total erythrocytes (PCEs + NCEs) and PCEs among NCEs were determined by analyzing 500 erythrocytes per animal. Moreover, the incidence of micronucleated polychromatic erythrocytes (MNPCE) was determined by scoring a minimum of 5000 PCEs per animal and the results were expressed as % of micronucleus (% of MN) [34].

Statistical analysis

The values were depicted as mean ± standard error mean (SEM). Statistical analysis was performed by ANOVA using GraphPad prism software (version 5) followed by Tukey's multiple comparison test. The variation of the data obtained was considered to be statistically significant when $p < 0.05$.

Results

Characterization of complex

The UV–visible spectroscopy of fisetin and the complex has been demonstrated in Fig. 2A. The UV spectrum of fisetin showed two visible bands in 360 nm (band I) and 268 nm (band II).The fisetin ruthenium-p-cymene complex resulted in the shifting of band I and band II at 436 nm (band III) and 320 nm (band IV) respectively. The IR spectroscopic data of fisetin and complex has been depicted in Table 1 and Fig. 2B, which represented the distinguishing bands of fisetin and fisetin ruthenium-p-cymene complex. The IR spectrum of fisetin demonstrated the formation of *V*(O–H) band at 3361.49 for fisetin is shifted to 3350.58 after complexation. The *V*(C = O) band stretching for fisetin occurs at 1607.60 cm^{-1} which was slightly shifted to 1608.13 cm^{-1} for the complex. The bands which were detected at 1255.90 cm^{-1} and 1104.45 cm^{-1} represent the shift for *V(C–OH)* and *V(C–O–C)* for fisetin which were slightly shifted to 1279.69 cm^{-1} and 1118.28 cm^{-1} respectively in complex. Moreover, a distinguishable peak *V*(RU–O) was observed for the complex at the region of 558.46 cm^{-1} which was absent in the FTIR spectrum of fisetin. The mass spectroscopy was depicted in Fig. 2C.The molecular ion peak of the complex with m/z 556.05. The surface morphological features of the complex were depicted through scanning electron microscopy at different magnifications (Fig. 2D–G).

Radical scavenging activity of fisetin and fisetin ruthenium-p-cymene complex by DPPH method

Fisetin is a bioflavonoid that is widely known for its potent ability to scavenge free radicals and form chelates with different transition metals. The natural capacity of the complex to scavenge free radicals is altered by the formation of metal and flavonoid complex cations, indicating that the complex

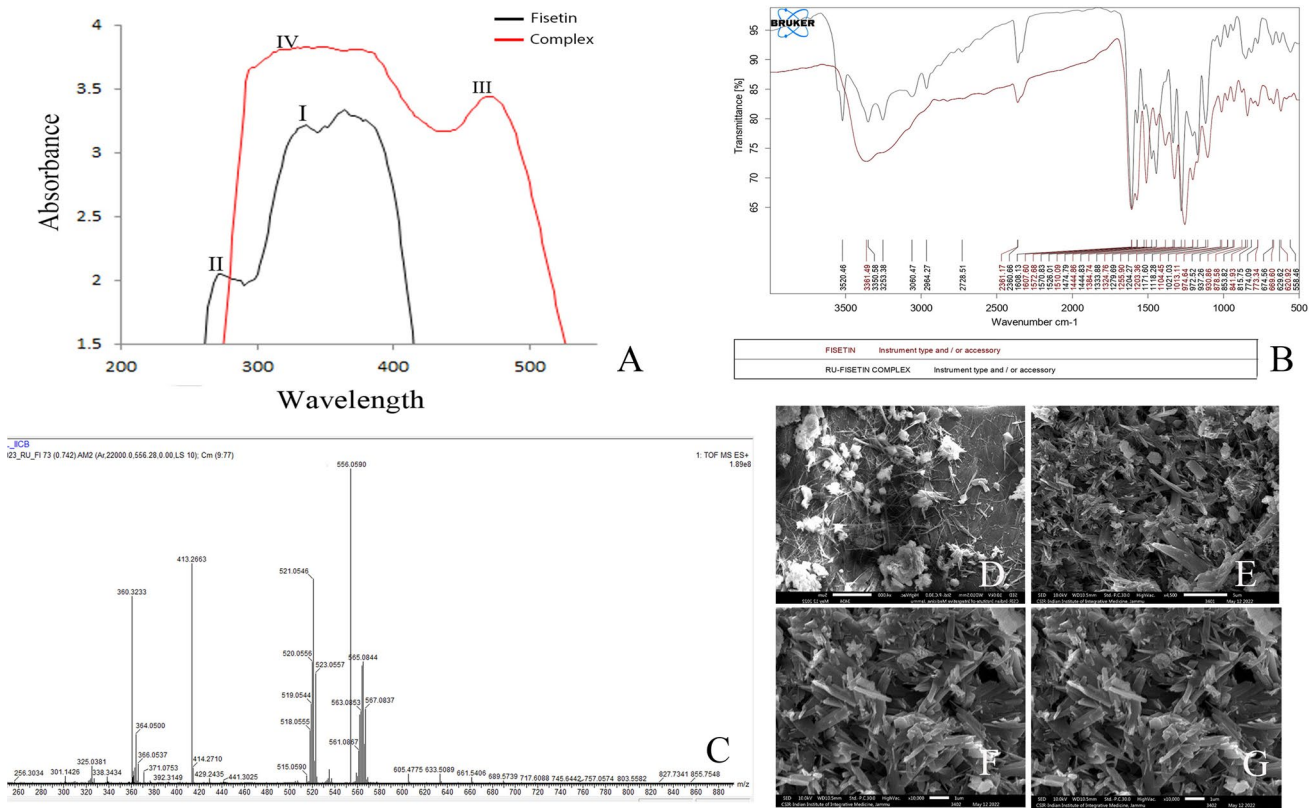

Fig. 2 **A** UV–visible spectra of fisetin and fisetin ruthenium-p-cymene complex. **B** FT-IR spectra of fisetin ruthenium-p-cymene complex. **C** Mass spectra of fisetin ruthenium-p-cymene complex showing molecular ion peaks. Scanning electron microscopic images of the complex at **D** 4000X **E** 4500X **F** 6000X **G** 10,000X magnification

Table 1 IR Spectroscopy band position

Compound	*V*(O–H)	*V*(C = O)	*V*(C = = C)	*V*(C–OH)	*V*(C–O–C)	*V*(M–O)
Fisetin	3361.49	1607.60	1444.86	1255.90	1104.45	–
Complex	3350.58	1608.13	1474.79	1279.69	1108.28	558.48

has changed free radical scavenging ability. The DPPH test demonstrates that antioxidants have the inherited ability to change the color of the DPPH radical from violet to yellow diphenyl-picryl-hydrazine. The antioxidants change the DPPH radical into the DPPH-H radical by adding a hydrogen atom to it. Therefore, the antioxidant activity of both flavonoid and metal flavonoid complex has been assessed using the DPPH radical scavenging method. The absorption spectra of different DPPH solution containing different concentration of free fisetin and the complex has been depicted in (Fig. 3A). The % radical scavenging activity (% RSA) of free fisetin increases very slightly with increasing concentration and the maximum % RSA is detected to be 99.06%. But for the complex it shows increase in the % RSA with increasing concentration and reaches up to 98.28%. The complex shows less DPPH radical scavenging activity than the free fisetin at same concentration.

Radical scavenging activity of fisetin and fisetin ruthenium-p-cymene complex by FRAP method

The FRAP antioxidant assay measures an antioxidant capacity to decrease Fe^{3+} to Fe^{2+} in the presence of TPTZ. After 10 min of the subject compound interaction with the FRAP reagent, the absorbance of fisetin and the fisetin ruthenium-p-cymene complex in the presence of Fe^{3+}-TPTZ was measured at 593 nm. The antioxidant content has an impact on the absorbance decrease. Figure 3B demonstrates that the complex has more antioxidant capacity than free fisetin.

Radical scavenging activity of fisetin and fisetin ruthenium-p-cymene complex by ABTS method

The anti-radical potential of the complex has been investigated by ABTS radical scavenging method. Figure 3C shows

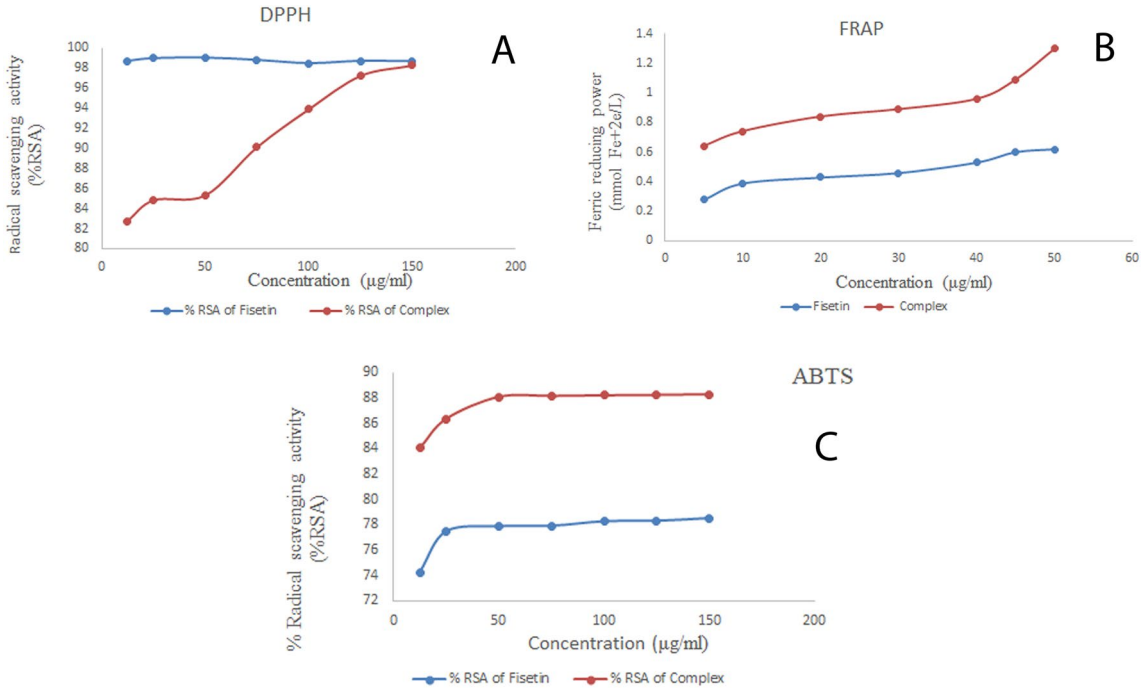

Fig. 3 Measurement of antioxidant activity of the complex. **A** DPPH method **B** FRAP method **C** ABTS method

that fisetin and the fisetin ruthenium-p-cymene complex have ABTS radical scavenging properties. In the presence of various concentrations of the complex, it was discovered that the absorption of active ABTS solution at 734 nm dramatically decreased. The complex was found to have more ABTS radical scavenging activity than free fisetin.

Toxicity study

The LD_{50} concentration of the fisetin ruthenium-p-cymene complex was determined as 500 mg/kg body weight. Subsequently, the sub-acute doses were determined as 50, 100, 200, and 400 mg/kg. The treatment with fisetin ruthenium-p-cymene complex was not associated with any treatment-related mortality.

Body weight and water consumption

The mean body weight and water consumption rate of the animals have been demonstrated in Fig. 4. The mean body weight and water consumption rate of animals in the 400 mg/kg group were significantly reduced as compared to the control and other complex treated groups.

Hematology and serum biochemistry

The hematological parameters mainly WBC count was significantly increased in the 400 mg/kg complex treated group as compared to the control group (Tables 2, 3). The serum biochemical analysis demonstrated a significant upregulation of ALT, AST, and ALP levels in the 400 mg/kg group as compared to other complex treated groups (Tables 4, 5). In addition, the levels of blood glucose and blood urea nitrogen were significantly enhanced in the 400 mg/kg group.

Gross observation and organ weight

The weight of the essential organs i.e. the stomach, kidney, lung, pancreas, liver, testis, and ovary, were investigated after the 28-day repeated dose toxicity trial. There were no such noteworthy changes observed in the absolute and relative weight of the organs in the 50, 100, and 200 mg/kg groups. Whereas, in the 400 mg/kg treated group a significant increase in the absolute and relative weight of the organs was detected (Fig. 5).

Histopathology

The vital organ of the animals were analyzed for histopathology after sub-acute toxicity study. In the control group, the tissue morphology of mice liver showed the central vein (cv), portal vein (pv), hepatic artery (ha), bile duct (bd), sinusoids (s), lymph vessel (lv), hepatocytes (h), and kuffer cells (kc) (Fig. 6(i)A), whereas 400 mg/kg (Fig. 6(i)E) dose animals showed periportal mononeuclear infiltrates (pmi), hepatocytes degeneration (hd), sinusoidal dialation (sd) and focal inflammation (fi).The 50, 100, 200 mg/kg group did not depicted any toxicological

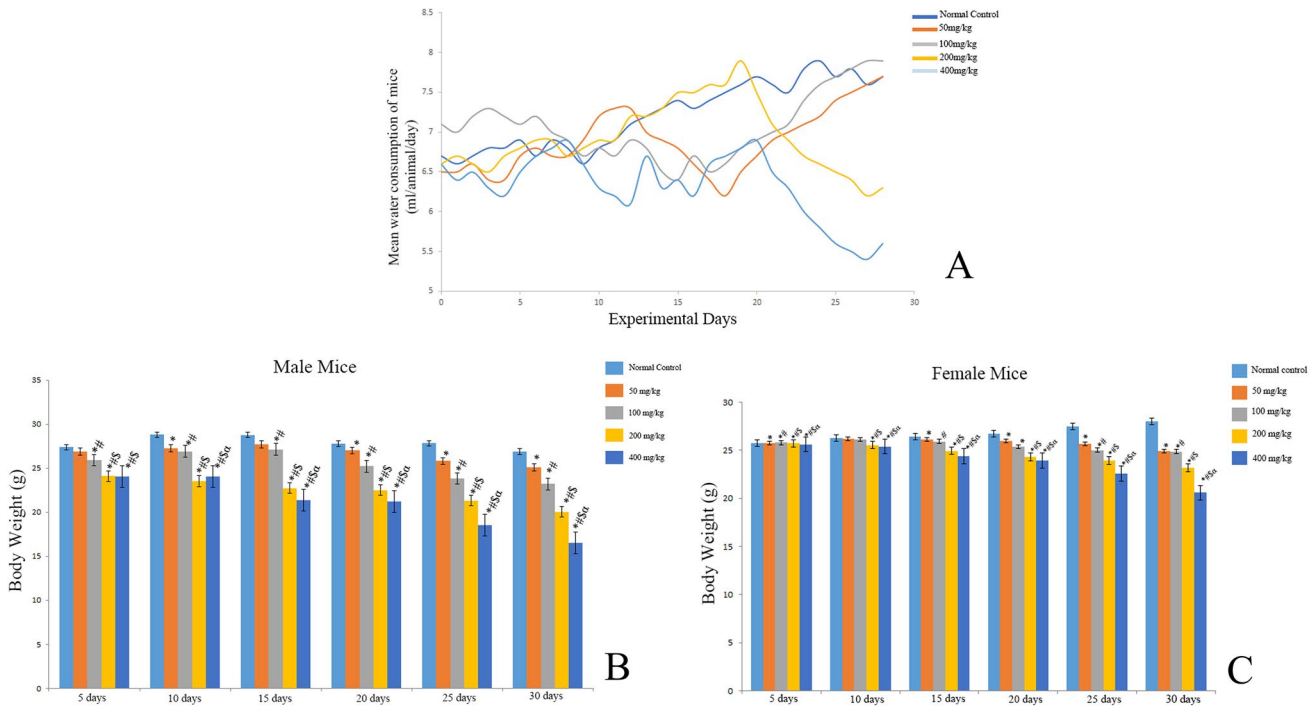

Fig. 4 **A** Graphical representation of mean water consumption of mice. Bar diagram graph of mean body weight of **B** Male mice and **C** Female mice. *Represented $p < 0.05$ as compared to normal control. Similarly # represented $p < 0.05$ as compared to 50 mg/kg group, $ $p < 0.05$ as compared to 100 mg/kg group, α $p < 0.05$ as compared to 200 mg/kg group. Data represent means ± SEM (n = 6). The results were compared using ANOVA, followed by a Tukey's multiple comparison post-hoc analysis

Table 2 Hematological finding in male Swiss albino mice treated with fisetin ruthenium-p-cymene complex for 28 days repeated-dose oral subacute toxicity study

Parameters (± SEM)	Control	Fisetin ruthenium-p-cymene (50 mg)	Fisetin ruthenium-p-cymene (100 mg)	Fisetin ruthenium-p-cymene (200 mg)	Fisetin ruthenium-p-cymene (400 mg)
Total RBC (10^6/μL)	4.30 ± 0.005	4.37 ± 0.006*	4.43 ± 0.004$^{*\#}$	4.66 ± 0.007$^{*\#\$}$	5.08 ± 0.0253$^{*\#\$\alpha}$
Hemoglobin (%)	12.24 ± 0.004	12.25 ± 0.005	12.33 ± 0.018$^{*\#}$	12.57 ± 0.006$^{*\#\$}$	13.52 ± 0.008$^{*\#\$\alpha}$
Platelet count (10^5/μL)	2.93 ± 0.009	2.75 ± 0.012*	2.85 ± 0.006$^{*\#}$	2.67 ± 0.011$^{*\#\$}$	4.37 ± 0.006$^{*\#\$\alpha}$
WBC (10^3/ μL)	8.85 ± 0.011	6.60 ± 0.030*	6.58 ± 0.024$^{*\#}$	7.82 ± 0.02$^{*\#\$}$	13.38 ± 0.08$^{*\#\$\alpha}$
MCV (fL)	91.04 ± 0.18	88.68 ± 0.06*	87.60 ± 0.19$^{*\#}$	87.68 ± 0.16$^{*\#}$	92.69 ± 0.11$^{*\#\$\alpha}$
MCH (pg)	28.65 ± 0.09	29.16 ± 0.06*	29.41 ± 0.09*	25.49 ± 0.14$^{*\#\$}$	29.81 ± 0.08$^{*\#\$\alpha}$
MCHC (%)	33.26 ± 0.006	31.55 ± 0.009*	30.26 ± 0.008$^{*\#}$	31.85 ± 0.01$^{*\#\$}$	31.65 ± 0.01$^{*\#\$\alpha}$
Neutrophil (%)	28.20 ± 0.22	25.18 ± 0.008*	27.38 ± 0.02$^{*\#}$	25.24 ± 0.01$^{*\$}$	30.12 ± 0.02$^{*\#\$\alpha}$
Eosinophil (%)	11.76 ± 0.01	17.03 ± 0.01*	24.15 ± 0.008$^{*\#}$	36.53 ± 0.01$^{*\#\$}$	65.70 ± 0.02$^{*\#\$}$
Monocytes (%)	1.17 ± 0.01	2.19 ± 0.02*	1.21 ± 0.02$^{\#}$	1.29 ± 0.01$^{*\#\$}$	2.20 ± 0.01$^{*\$\alpha}$
Basophil (%)	0.0 ± 0.0	0.0 ± 0.0	0.0 ± 0.0	0.0 ± 0.0	0.0 ± 0.0

Standard error of mean = standard deviation (SD)/$\sqrt{}$ Total subject. Result are analyzed by one-way ANOVA and confirmed by Tukey's post-hoc multiple comparison analysis

MCV mean corpuscular volume, *MCH* mean corpuscular hemoglobin, *MCHC* mean corpuscular hemoglobin concentration, *RBC* red blood cell, *WBC* white blood cell

*Significant difference at $p < 0.05$, when compared with control group

#Significant difference at $p < 0.05$, when compared with 50 mg/kg group

$Significant difference at $p < 0.05$, when compared with 100 mg/kg group

αSignificant difference at $p < 0.05$, when compared with 200 mg/kg group

Table 3 Hematological finding in female Swiss albino mice treated with fisetin ruthenium-p-cymene complex for 28 days repeated-dose oral sub-acute toxicity study

Parameters	Control	Fisetin ruthenium-p-cymene (50 mg)	Fisetin ruthenium-p-cymene (100 mg)	Fisetin ruthenium-p-cymene (200 mg)	Fisetin ruthenium-p-cymene (400 mg)
Total RBC (10^6/μL)	5.29 ± 0.01	4.67 ± 0.01*	4.38 ± 0.01$^{*\#}$	4.46 ± 0.05$^{*\#}$	5.12 ± 0.02$^{*\#\$\alpha}$
Hemoglobin (%)	13.28 ± 0.01	13.14 ± 0.01*	12.26 ± 0.01$^{*\#}$	12.67 ± 0.01$^{*\#\$}$	13.50 ± 0.02$^{*\#\$\alpha}$
Platelet count (10^5/μ)	2.94 ± 0.01	2.85 ± 0.009*	2.70 ± 0.02$^{*\#}$	2.72 ± 0.03$^{*\#}$	3.27 ± 0.009$^{*\#\$\alpha}$
WBC (10^3/L)	8.85 ± 0.01	5.18 ± 0.009*	6.76 ± 0.04*	6.85 ± 1.11$^{*\#\$}$	13.25 ± 0.01$^{*\#\$}$
MCV (fL)	88.77 ± 0.03	87.16 ± 0.01*	88.94 ± 0.01$^{*\#}$	86.36 ± 0.03$^{*\#\$}$	90.33 ± 0.03$^{*\#\$\alpha}$
MCH (pg)	28.27 ± 0.01	27.76 ± 0.008*	27.21 ± 0.01$^{*\#}$	29.17 ± 0.01$^{*\#\$}$	31.15 ± 0.02$^{*\#\$\alpha}$
MCHC (%)	33.19 ± 0.02	33.51 ± 0.07*	31.27 ± 0.006$^{*\#}$	30.64 ± 0.04$^{*\#\$}$	30.71 ± 0.02$^{*\#\$}$
Neutrophil (%)	28.55 ± 0.10	24.08 ± 0.009*	26.64 ± 0.11$^{*\#}$	25.76 ± 0.01$^{*\#\$}$	25.76 ± 0.008$^{*\#\$}$
Eosinophil (%)	2.15 ± 0.01	1.06 ± 0.01*	5.12 ± 0.02$^{*\#}$	6.08 ± 0.01$^{*\#\$}$	6.14 ± 0.02$^{*\#\$\alpha}$
Monocytes (%)	1.11 ± 0.01	2.12 ± 0.02*	1.05 ± 0.008$^{\#}$	1.07 ± 0.01$^{\#}$	2.08 ± 0.01$^{*\$\alpha}$
Basophil (%)	0.0 ± 0.0	0.0 ± 0.0	0.0 ± 0.0	0.0 ± 0.0	0.0 ± 0.0

Standard error of mean = standard deviation (SD)/$\sqrt{}$ Total subject. Result are analyzed by one-way ANOVA and confirmed by Tukey's post-hoc multiple comparison analysis

MCV mean corpuscular volume, *MCH* mean corpuscular hemoglobin, *MCHC* mean corpuscular hemoglobin concentration, *RBC* red blood cell, *WBC* white blood cell

*Significant difference at $p < 0.05$, when compared with control group

#Significant difference at $p < 0.05$, when compared with 50 mg/kg group

$Significant difference at $p < 0.05$, when compared with 100 mg/kg group

αSignificant difference at $p < 0.05$, when compared with 200 mg/kg group

Table 4 Serum biochemistry findings in male Swiss albino mice treated with fisetin ruthenium-p-cymene complex for 28 days repeated-dose oral sub-acute toxicity study

Parameters	Control	Fisetin ruthenium-p-cymene (50 mg)	Fisetin ruthenium-p-cymene (100 mg)	Fisetin ruthenium-p-cymene (200 mg)	Fisetin ruthenium-p-cymene (400 mg)
Aspartate aminotransferase (AST) (U/L)	39.14 ± 0.12	33.17 ± 0.01*	35.56 ± 0.01$^{*\#}$	41.07 ± 0.008$^{*\#\$}$	50.1 ± 0.02$^{*\#\$\alpha}$
Alanine aminotransferase (ALT) (U/L)	31.28 ± 0.01	34.22 ± 0.02*	37.46 ± 0.01$^{*\#}$	44.53 ± 0.02$^{*\#\$}$	52.07 ± 0.01$^{*\#\$\alpha}$
Alkaline phosphatase (ALP) (U/L)	357 ± 0.03	225 ± 0.07*	365 ± 0.06$^{*\#}$	357 ± 0.19$^{*\#\$}$	498 ± 0.01$^{*\#\$\alpha}$
Blood urea nitrogen (mg/dL)	17.17 ± 0.01	17.17 ± 0.01	18.46 ± 0.01$^{*\#}$	28.43 ± 0.02$^{*\#\$}$	30.19 ± 0.03$^{*\#\$\alpha}$
Creatinine (mg/dL)	0.65 ± 0.01	0.56 ± 0.006*	0.57 ± 0.01*	0.62 ± 0.01$^{*\#\$}$	0.72 ± 0.01$^{*\#\$}$
Glucose (mg/dL)	113.7 ± 0.07	103.1 ± 0.04*	112.6 ± 0.18$^{*\#}$	118.3 ± 0.08$^{*\#\$}$	131.8 ± 0.09$^{*\#\$\alpha}$
Cholesterol(mg/dL)	47.27 ± 0.01	43.27 ± 0.03*	46.23 ± 0.02$^{*\#}$	48.16 ± 0.009$^{*\#\$}$	52.11 ± 0.01$^{*\#\$\alpha}$

Standard error of mean = standard deviation (SD)/$\sqrt{}$ Total subject. Result are analyzed by one-way ANOVA and confirmed by Tukey's post-hoc multiple comparison analysis

*Significant difference at $p < 0.05$, when compared with control group

#Significant difference at $p < 0.05$, when compared with 50 mg/kg group

$Significant difference at $p < 0.05$, when compared with 100 mg/kg group

αSignificant difference at $p < 0.05$, when compared with 200 mg/kg group

alterations of liver tissue (Fig. 6(i)B-D). The kidney tissue (Fig. 6(ii)A) of the control group displayed the normal structure of the Glomerulus (g), Bowman's capsule (bc), proximal convoluted tubule (pct), distal convoluted tubule (dct), macula densa (md), juxtaglomerular cells (jgc), podocytes (p), vascular pole (vp), urinary pole (up) and mensangial cells (mc). The 50, 10, 200 mg/kg showed no such significant alteration of kidney (Fig. 6(ii) B-D). On the other hand, 400 mg/kg complex treated group depicted hemorrhages (h), thickening of the capsular membrane, desquamation of the epithelial cells (dec), vascular congestion (vc) and infiltration of inflammatory cells (iic)

Table 5 Serum biochemistry findings in female Swiss albino mice treated with fisetin ruthenium-p-cymene complex for 28 days repeated-dose oral sub-acute toxicity study

Parameters (± SEM)	Control	Fisetin ruthenium-p-cymene (50 mg)	Fisetin ruthenium-p-cymene (100 mg)	Fisetin ruthenium-p-cymene (200 mg)	Fisetin ruthenium-p-cymene (400 mg)
Aspartate aminotransferase (AST) (U/L)	31.26 ± 0.008	32.18 ± 0.01*	33.10 ± 0.47$^{*\#}$	40.12 ± 0.02$^{*\#\$}$	50.08 ± 0.02$^{*\#\$\alpha}$
Alanine aminotransferase (ALT) (U/L)	31.26 ± 0.01	35.07 ± 0.02*	46.51 ± 0.05$^{*\#}$	37.54 ± 0.04$^{*\#\$}$	50.07 ± 0.01$^{*\#\$\alpha}$
Alkaline phosphatase (ALP) (U/L)	351.5 ± 0.09	221.5 ± 0.04*	316.5 ± 0.09$^{*\#}$	385.3 ± 1.24$^{*\#\$}$	401.5 ± 0.12$^{*\#\$\alpha}$
Blood urea nitrogen (mg/dL)	18.15 ± 0.01	18.05 ± 0.01	28.59 ± 0.06$^{*\#}$	28.56 ± 0.01$^{*\#}$	30.16 ± 0.006$^{*\#\$\alpha}$
Creatinine (mg/dL)	0.65 ± 0.012	0.55 ± 0.01*	0.58 ± 0.007*	0.67 ± 0.008$^{\#\$}$	0.69 ± 0.01$^{\#\$}$
Glucose (mg/dL)	115.5 ± 0.09	128.6 ± 0.07*	117.5 ± 0.10$^{*\#}$	113.5 ± 0.13$^{*\#\$}$	127.5 ± 0.07$^{*\#\$\alpha}$
Cholesterol(mg/dL)	47.16 ± 0.01	44.08 ± 0.01*	45.16 ± 0.04$^{*\#}$	47.20 ± 0.06$^{\#\$}$	50.19 ± 0.02$^{*\#\$\alpha}$

Standard error of mean = standard deviation (SD)/$\sqrt{}$ Total subject. Result are analyzed by one-way ANOVA and confirmed by Tukey's post-hoc multiple comparison analysis

*Significant difference at $p < 0.05$, when compared with control group

$^{\#}$Significant difference at $p < 0.05$, when compared with 50 mg/kg group

$^{\$}$Significant difference at $p < 0.05$, when compared with 100 mg/kg group

$^{\alpha}$Significant difference at $p < 0.05$, when compared with 200 mg/kg group

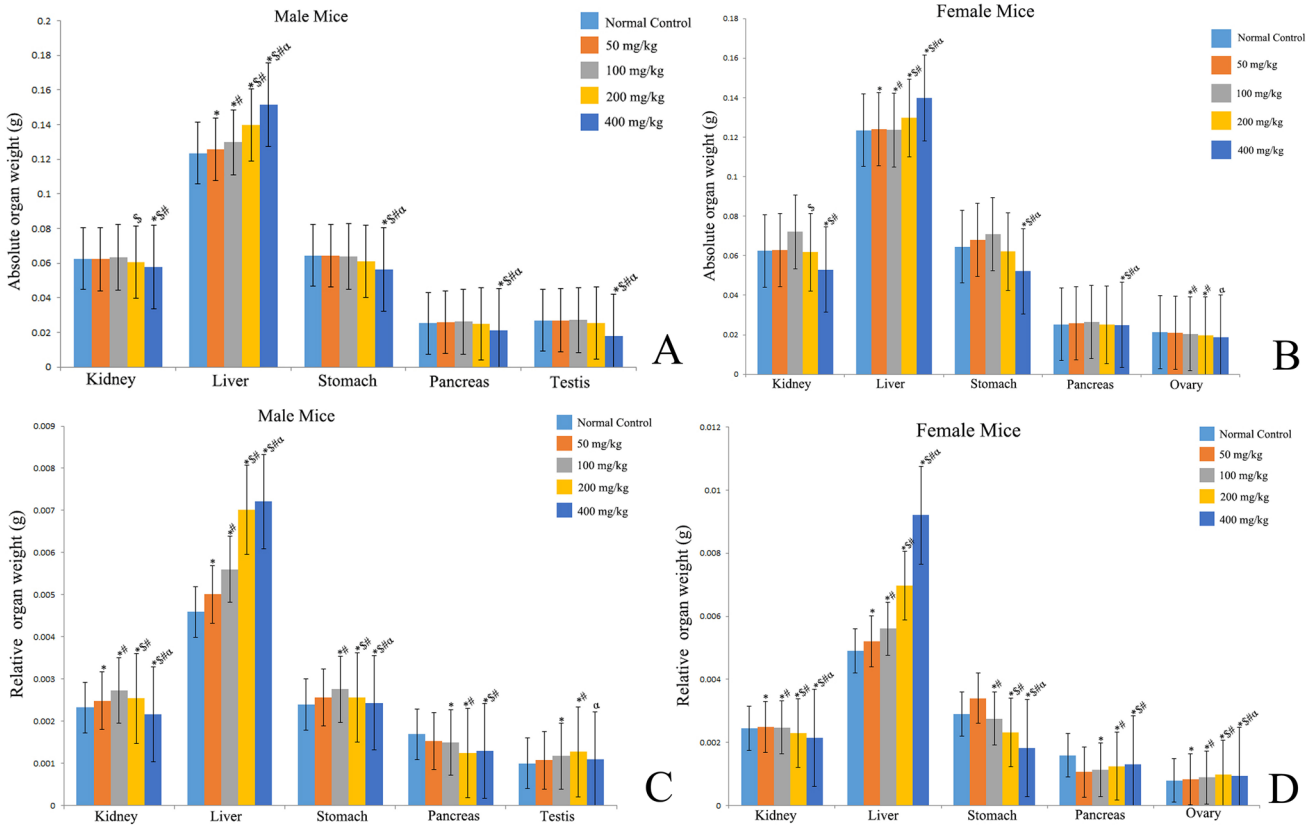

Fig. 5 Bar diagram depicting absolute organ weight of **A** Male mice and **B** Female mice. Bar diagram depicting relative organ weight of **C** Male mice and **D** Female mice. *Represented $p < 0.05$ as compared to normal control. Similarly # represented $p < 0.05$ as compared to 50 mg/kg group, $ $p < 0.05$ as compared to 100 mg/kg group, α $p < 0.05$ as compared to 200 mg/kg group. Data represent means ± SEM (n = 6). The results were compared using ANOVA, followed by a Tukey's multiple comparison post-hoc analysis

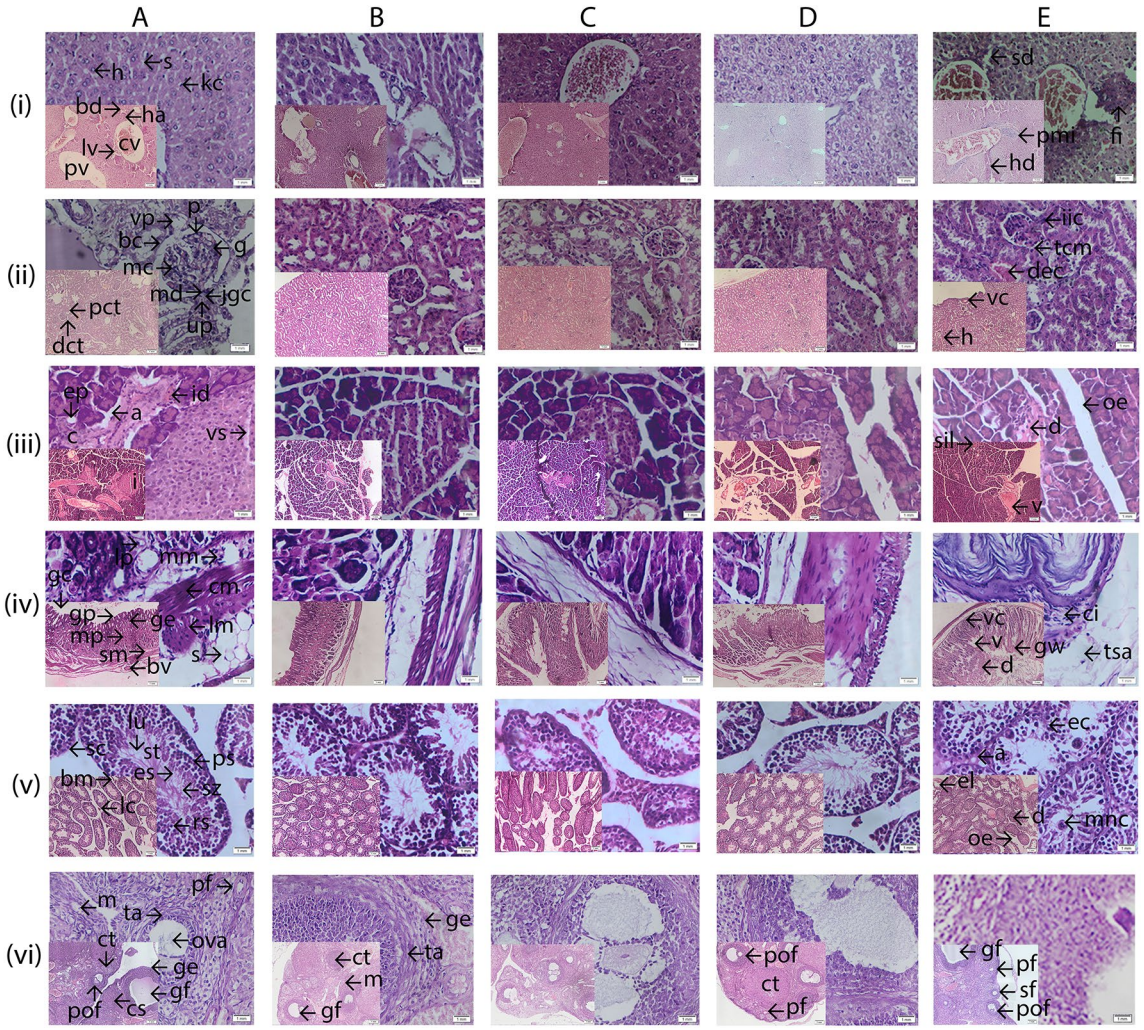

Fig. 6 Histopathological representation of (i) Liver (ii) Kidney (iii) Pancreas (iv) Stomach (v) Testis, and (vi) Ovary of Swiss albino mice where **A** Control group **B** 50 mg/kg complex treated group **C** 100 mg/kg complex treated group **D** 200 mg/kg complex treated group **E** 400 mg/kg complex treated group. Control group of liver showing central vein (cv), portal vein (pv), bile duct (bd), hepatic artery (ha), sinusoids (s), lymph vessel (lv), hepatocytes (h), and kuffer cells (kc). 400 mg/kg complex of liver showing periportal mononeuclear infiltrates (pmi), hepatocytes degeneration (hd), sinusoidal dialation (sd) and focal inflammation (fi). Control group of kidney showing glomerulus (g), Bowman's capsule (bc), proximal convoluted tubule (pct), distal convoluted tubule (dct), macula densa (md), juxtaglomerular cells (jgc), podocytes (p), vascular pole (vp), urinary pole (up) and mensangial cells (mc). 400 mg/kg complex group of kidney showing haemorrhages (h), thickening of the capsular membrane(tcm),desquamation of the epithelial cells (dec), vascular congestion (vc) and infiltration of inflammatory cells (iic). Control group of pancreas showing islets of Langerhans (i), normal acinar arrangements with basal basophila and apical acidophila (a), exocrine portion (ep), collagen (c), intralobular duct (id) and vascular stroma (vs). 400 mg/kg complex group of pancreas showing oedema (oe), shrinkage of islet of Langerhans (sil), degenerated entrapped islet of Langerhans (d) and vacuolization (v). Control group of stomach showing muscularis mucosa (mm), submucosa (sm), lamina propia (lp), gastric pits (gp), gastric cavity (gc), gastric epithelium (ge), muscularis propia (mp), circular muscle (cm), longitudinal muscle (lm), serosa (s) and blood vessels (bv). 400 mg/kg complex group of stomach showing vascular congestion (vc), thickening of the submucosal area (tsa), cellular infiltration (ci), desquamation of gastric mucosa (d), vacuolization (v) and glandular widening (gw). Control group of testis showing seminiferous tubules (st), sertoli cells (sc), primary spermatocyte (ps), spermatozoa (sz), leydig cells (lc) lumen (lu), round spermatids (rs), elongated spermatid (es) and basement membrane (bm). 400 mg/kg complex group of testis showing degeneration of seminiferous tubules (d),edema in intestinal tissue (oe), vacuolization (v),exfoliated cells (ec), empty lumen (el), atrophy of leydig cells (a) and multinucleated giant cells (mnc). Control group of ovary showing germinal epithelium (ge), tunica albuginea (ta), graafian follicle (gf), corpus lutea (ct), preovulatory follicle (pof), ova, cortical stroma (cs), primordial follicle (pf), medulla (m), and secondary follicle (sf). 400 mg/kg complex treated group showing no significant alteration. (H&E) 10X magnification [inset 40X]

(Fig. 6(ii)E). The control group depicted normal histopathology of the pancreas (Fig. 6(i) A) which include islets of Langerhans (i), normal acinar arrangements with basal basophila and apical acidophila (a), exocrine portion (ep), collagen (c), intralobular duct (id) and vascular stroma (vs). Pancreatic tissue of 400 mg/kg group (Fig. 6(iii)E) showed oedema (oe), shrinkage of islet of Langerhans (sil), degenerated entrapped islet of Langerhans (d) and vacuolization (v). The 50,100,200 mg/kg group did not show any histological alteration of pancreas (Fig. 6(iii) B-D).The stomach tissue of control group showed muscularis mucosa (mm), submucosa (sm), lamina propia (lp), gastric pits (gp), gastric cavity (gc), gastric epithelium (ge), muscularis propia (mp), longitudinal muscle (lm), circular muscle (cm), serosa (s) and blood vessels (bv) (Fig. 6(iv)A). The 50, 100, 200 mg/kg group did not exerted `any toxicological alteration of stomach tissue (Fig. 6(iv) B-D). Whereas 400 mg/kg treated group marked structural alterations such as vascular congestion (vc), thickening of the submucosal area (tsa), cellular infiltration (ci), desquamation of gastric mucosa (d), vacuolization (v) and glandular widening (gw) (Fig. 6(iv) E). The control group illustrated normal histopathology of the testis (Fig. 6(v)A) which include seminiferous tubules (st), sertoli cells (sc), primary spermatocyte (ps), spermatozoa (sz), leydig cells (lc) lumen (lu), round spermatids (rs), elongated spermatid (es) and basement membrane (bm). Animals of 50,100 and 200 mg/kg group showed no marked alteration (Fig. 6(v)B-D), whereas the 400 mg/kg treated group depicted degeneration of seminiferous tubules (d), edema in intestinal tissue (oe), vacuolization (v), exfoliated cells (ec), empty lumen (el), atrophy of leydig cells (a) and multinucleated giant cells (mng) (Fig. 6(v)E). The control group of Swiss albino mice ovary showed normal histological architecture which includes tunica albuginea (ta), germinal epithelium (ge), graafian follicle (gf), corpus lutea (ct), preovulatory follicle (pof), ova, cortical stroma (cs), primordial follicle (pf), medulla (m), and secondary follicle (sf) (Fig. 6(vi) A). Animals in groups 50, 100, 200, and 400 mg/kg displayed no distingusible alteration compared to the vehicle control group (Fig. 6(vi)B-E).

Ames test

The result of mutagenicity testing has been demonstrated in Table 6. The positive control chemical demonstrated a significant upregulation of mutant colonies in comparison to vehicle control group which suggested the sensitivity of the system. Conversely, the 5 and 10 mg/plate complex treated group did not showed any noticeable difference in the number of mutant colonies. The 20 and 40 mg/plate group showcased a significant inhibition of proliferation of Salmonella strains irrespective of S9 mediated metabolic activity.

Chromosomal aberration test

The chromosomal aberration was detected by evaluating using 150 well separated metaphase cells for any chromosomal abnormality (Fig. 7(i), Table 7). The chromosomal aberration was considered according to different parameters which include breakage of fragments, ring formation, polyploidy, aneuploidy, and deletion. The cyclophosphamide treated group (Fig. 7(i)B-E) depicted significant chromosomal aberration, whereas the treatment with the fisetin ruthenium-p-cymene complex at different concentration (50,100,200, and 400 mg/kg) was not related to any chromosomal aberration (Fig. 7(i)A).

Micronucleus assay

The result of the micronucleus assay has been depicted in the (Fig. 7(ii) and Table 8). The cyclophosphamide treated group demonstrated a significant upregulation in the PCE/Total erythrocyte, PCE/NCE in comparison to the vehicle control group. Additionally, a significant reduction of % MN

Table 6 Ames test result of fisetin ruthenium-p-cymene complex

Liver extract	Vehicle control	Positive control	5 mg/plate complex	10 mg/plate complex	20 mg/plate complex	40 mg/plate complex
$S9^+$	36.87 ± 0.8	1857.47 ± 0.67*	35.53 ± 0.4$^{\#}$	34.9 ± 0.17$^{\#}$	17.63 ± 0.52*$^{\#\$\alpha}$	4.27 ± 0.39*$^{\#\$\alpha\beta}$
$S9^-$	38.33 ± 0.49	1792.53 ± 0.49*	37.97 ± 0.38$^{\#}$	37.37 ± 0.49$^{\#}$	19.53 ± 0.64*$^{\#\$\alpha}$	5.27 ± 0.38*$^{\#\$\alpha\beta}$

The assays were performed in triplicate manner. The values were depicted as mean ± SEM (n = 3). The results were compared using one-way ANOVA, followed by a Tukey's post-hoc multiple comparison analysis

*Significant difference as compared to the vehicle control group ($p < 0.05$)

$^{\#}$Significant difference as compared to the positive control group ($p < 0.05$)

$^{\$}$Significant difference as compared to the 5 mg/plate complex ($p < 0.05$)

$^{\alpha}$Significant difference as compared to the 10 mg/plate complex ($p < 0.05$)

$^{\beta}$Significant difference as compared to the 20 mg/plate complex ($p < 0.05$)

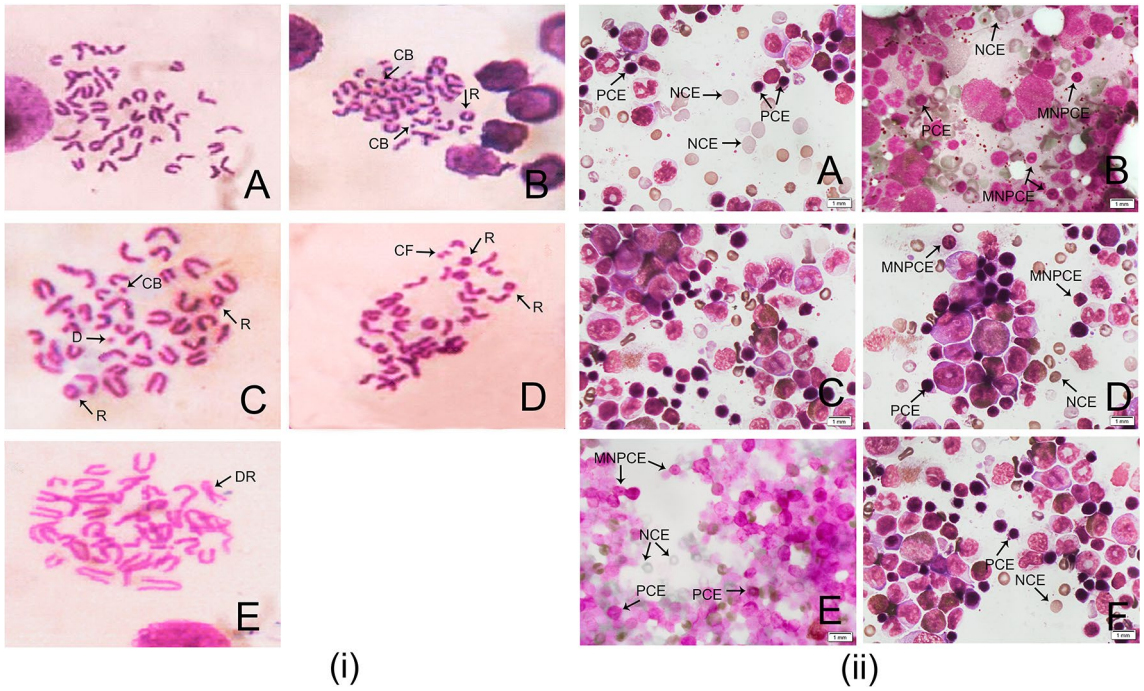

Fig. 7 **i** Chromosomal aberration tests **A** Normal metaphase. Cyclophosphamide treated group showing **B** Chromosome break (*CB*) and chromosomal ring formation (*R*) **C** Chromosome break (*CB*), chromosomal ring formation (*R*), and deletion (*D*) **D** Chromosomal fragmentation (*CF*) and ring formation (*R*) **E** Dicenteric ring formation (*DR*). **ii** Micronucleus assay **A** Vehicle control group **B** Cyclophosphamide treated group **C** 50 mg/kg complex **D** 100 mg/kg complex **E** 200 mg/kg complex **F** 400 mg/kg complex treated group. *PCE* polychromatic erythrocyte, *NCE* normochromatic erythrocyte, *MNPCE* micronucleated polychromatic erythrocyte

Table 7 Chromosomal aberration test

Sex	Treatment groups	Breakage/Fragments	Ring	Aneuploidy	Polyploidy	Deletion	Total aberration %
	Control	6.1	2.3	2.3	0.0	1.5	2.48 ± 0.01
	Cyclophosphamide (40 mg/kg)	50.65*	11.65*	4.05*	1.43	4.3*	14.13 ± 0.02*
Male	50 mg/kg complex	6.4$^{*\#}$	1.8$^{*\#}$	2.2$^{\#}$	0.0	0.48$^{*\#}$	2.20 ± 0.02$^{*\#}$
	100 mg/kg complex	5.6$^{*\#\$}$	1.7$^{*\#}$	1.7$^{*\#\$}$	0.0	0.33$^{*\#}$	1.88 ± 0.02$^{*\#\$}$
	200 mg/kg complex	6.05$^{\#\$\alpha}$	1.8$^{*\#}$	2.4$^{\#\alpha}$	0.0	0.73$^{*\#\alpha}$	2.20 ± 0.01$^{*\#\alpha}$
	400 mg/kg complex	6.08$^{\#\$\alpha}$	1.95$^{*\#\alpha}$	2.7$^{*\#\$\alpha\beta}$	0.0	0.81$^{*\#\$\alpha}$	2.31 ± 0.02$^{*\#\$\alpha\beta}$
	Control	6.2	1.9	2.1	0.0	1.7	2.39 ± 0.01
	Cyclophosphamide (40 mg/kg)	51.3*	12.41*	4.3*	1.41	4.5*	14.53 ± 0.01*
Female	50 mg/kg complex	5.8$^{*\#}$	1.75$^{\#}$	2.25$^{\#}$	0.0	0.36$^{*\#}$	2.04 ± 0.02$^{*\#}$
	100 mg/kg complex	5.8$^{*\#}$	1.75$^{\#}$	1.73$^{*\#\$}$	0.0	0.53$^{*\#}$	1.9 ± 0.02$^{*\#}$
	200 mg/kg complex	5.7$^{*\#}$	1.73$^{\#}$	2.75$^{*\#\$\alpha}$	0.0	0.85$^{*\#\$\alpha}$	2.2 ± 0.02$^{*\#\$\alpha}$
	400 mg/kg complex	5.8$^{*\#}$	1.8$^{\#}$	2.8$^{*\#\$\alpha}$	0.0	0.94$^{*\#\$\alpha}$	2.27 ± 0.03$^{*\#\$\alpha}$

Data expressed as mean ± SEM (n = 6). The results were compared using one-way ANOVA, followed by a Tukey's post-hoc multiple comparison analysis

*Significant difference as compared to the vehicle control group ($p < 0.05$)

$^{\#}$Significant difference as compared to the positive control group ($p < 0.05$)

$^{\$}$Significant difference as compared to the 50 mg/kg complex ($p < 0.05$)

$^{\alpha}$Significant difference as compared to the 100 mg/kg complex ($p < 0.05$)

$^{\beta}$Significant difference as compared to the 200 mg/kg complex ($p < 0.05$)

Table 8 Bone marrow micronucleus assay

Treatment groups	PCE/Total		PCE/NCE		%MN	
	Male	Female	Male	Female	Male	Female
Vehicle control	1.08 ± 0.001	1.07 ± 0.003	1.04 ± 0.003	1.02 ± 0.0006	4.20 ± 0.002	4.06 ± 0.03
Cyclophosphamide	0.68 ± 0.001*	0.53 ± 0.003*	0.67 ± 0.002*	0.47 ± 0.003*	35.3 ± 0.02*	35.02 ± 0.007*
50 mg/kg complex	1.16 ± 0.001$^{*\#}$	1.12 ± 0.002$^{*\#}$	1.05 ± 0.0008$^{*\#}$	1.04 ± 0.0008$^{*\#}$	5.68 ± 0.05$^{*\#}$	5.2 ± 0.03$^{*\#}$
100 mg/kg complex	1.34 ± 0.002$^{*\#\$}$	1.32 ± 0.003$^{*\#\$}$	1.09 ± 0.001$^{*\#\$}$	1.074 ± 0.001$^{*\#\$}$	6.15 ± 0.03$^{*\#\$}$	5.73 ± 0.08$^{*\#\$}$
200 mg/kg complex	1.17 ± 0.003$^{*\$\alpha}$	1.14 ± 0.002$^{*\#\$\alpha}$	1.16 ± 0.008$^{*\#\$\alpha}$	1.12 ± 0.0008$^{*\#\$\alpha}$	6.81 ± 0.02$^{*\#\$\alpha}$	6.38 ± 0.04$^{*\#\$\alpha}$
400 mg/kg complex	1.26 ± 0.002$^{*\#\$\alpha\beta}$	1.04 ± 0.002$^{*\#\$\alpha\beta}$	1.22 ± 0.001$^{*\#\$\alpha\beta}$	1.17 ± 0.003$^{*\#\$\alpha\beta}$	5.3 ± 0.05$^{*\#\$\alpha\beta}$	6.91 ± 0.02$^{*\#\$\alpha\beta}$

Data expressed as mean ± SEM (n = 6).The results were compared using one-way ANOVA, followed by a Tukey's post-hoc multiple comparison analysis

Bone marrow cytotoxicity expressed as polychromatic erythrocytes (PCE) among total erythrocytes (normochromatic erythrocytes (NCE) + PCE), ratio PCE among NCE and the micronuclei induction expressed as % MN

*Significant difference as compared to the vehicle control group ($p < 0.05$)

$^{\#}$Significant difference as compared to the cyclophosphamide group ($p < 0.05$)

$^{\$}$Significant difference as compared to the 50 mg/kg complex ($p < 0.05$)

$^{\alpha}$Significant difference as compared to the 100 mg/kg complex ($p < 0.05$)

$^{\beta}$Significant difference as compared to the 200 mg/kg complex ($p < 0.05$)

was noted cyclophosphamide treated group in both sexes as compared to vehicle control group. However, the fisetin ruthenium-p-cymene complex treated group (50, 100, 200, and 400 mg/kg) was noted associated with any significant alteration of PCE/Total erythrocyte, PCE/NCE, and % of MN in either sex as compared to the vehicle control group.

Discussions

Flavonoids are one of those naturally occurring products that exhibit various biological events [35, 36]**.** Chelation of these flavonoids with suitable metal leads to increased activity of the flavonoid against various diseases [37]. We have synthesized a new metal complex and our present study is mainly associated with the investigation of the toxicological profiling of the fisetin ruthenium-p-cymene complex. In this research, the synthesis and characterization of fisetin ruthenium-p-cymene complex was carried out through the assessment of various spectroscopical techniques. The UV spectroscopical analysis demonstrated that maximum shifting occurs at the band I position of fisetin through n-π* transition due to the formation of the metal complex. These findings suggested that the complexation of fisetin with ruthenium-p-cymene occurred in the cinnamoyl moiety of fisetin at 3-hydroxy-4-oxo position. The FT-IR spectrum of the complex depicted the formation of the ruthenium oxide (Ru–O) bond at the 558.46 cm^{-1} region which was absent in the FT-IR spectrum of fisetin. Thus, the development of metal chelate with fisetin through the generation of ruthenium-oxide bond is confirmed. The mass spectroscopy analysis illustrated the molecular ion peak of the complex at m/z 556.05, which confirms the formation of the fisetin ruthenium-p-cymene complex. SEM images further demonstrated the surface morphology and the crystalline nature of the novel fisetin ruthenium-p-cymene complex.

Antioxidant property of several flavonoids is substantially linked to their molecular structure. Hydrogen atom transferring and electron donation are the two major mechanisms, through which the phenolic compounds exert their antioxidant activity. The co-ordination of flavonoids with metal ions enhances the antioxidant activity and change the free radical scavenging ability of fisetin. In our present study the fisetin ruthenium-p-cymene complex showed slightly less antioxidant potential than the free fisetin in DPPH but showed more antioxidant potential for FRAP and ABTS radical scavenging activity methods. This proves that after complexation of fisetin with ruthenium-p-cymene the electron donating ability of the fisetin has been enhanced which influences the antioxidant potential. Moreover, the proton donating ability of the complex abrogated the chain reaction and increased antioxidant efficacy due to greater ability of the hydroxyl groups to donate hydrogen atoms after being chelated with the ruthenium-p-cymene moiety.

Furthermore, the toxicological analysis of the novel organometallic complex was performed through acute and sub-acute oral toxicity studies. As per the acute toxicity study the LD_{50} of the complex was determined as 500 mg/kg. Subsequently, the sub-acute doses were determined as 50, 100, 200 and 400 mg/kg. The haematological and serum biochemical analysis suggested an increased level of ALT, AST, ALP, ALT, BUN, and WBC count in the 400 mg/kg group. Additionally, the histopathology of vital organs depicted significant toxicity in the 400 mg/kg group excluded ovary. The

other groups like 50, 100, and 200 mg/kg was not associated with any significant alteration of haematological, serum biochemical parameters as well as histopathological evaluation.

In addition, mutagenicity testing was carried out to identify the substances which caused genetic mutation in somatic and/or germ cells that may eventually lead to the onset of various diseases including cancer. Previous report has been suggested that the accumulation of large number of mutant genes and chromosomal anomalies are responsible for the development of cancer phenotype or drive the cells towards the formation of an overt cancer [38]. In view of the above, the mutagenic potential of the complex was investigated by the Ames test, a bacterial reverse mutation assay, has been particularly developed to identify a broad range of substances that might cause genomic alteration. In this test, the histidine-dependent salmonella strains (His^-) are unable to grow in histidine free medium. However, the salmonella tester strains can revert to histidine forming strains (His^+) in presence of mutagenic substance in the culture media which are known as revertant colonies. Several studies reported that, the test compounds that inhibit the proliferation of revertant colonies are non-mutagenic [39]. In this study, 20 and 40 mg/plate complex treated group significantly decreased the revertant colonies which signified potent antibacterial activity of the complex. Nevertheless, the 5 and 10 mg/plate groups were unable to inhibit the number of mutant colonies as these doses were tolerant by the bacterium. Taking together, there was no significant increment in the number of revertant colonies in any of the complex treated groups in the presence or absence of S9 which signifies that the ruthenium-p-cymene complex was not associated with any genetic mutation in prokaryotic cells.

Our research also carried out the genotoxicity testing to identify the genotoxic substance that can cause DNA or chromosomal damage, which leads to somatic mutation and malignant transformation [40]. The genotoxicity of compounds is generally assessed by the chromosomal aberration test which is used to detect the chromosomal damage by the test compounds. According to the OECD guideline TG-473, the chromosomal aberration of any substance is measured by various parameters such as aneuploidy, polyploidy, and deletion. Several studies reported that increase chromosomal aberration is directly associated with altered genetic sequencing and chromosomal damage [41]. In this study, the cyclophosphamide treated group exhibit a substantial increment in chromosomal aberration as compared to the vehicle control group which was in accord with the previous findings by Ghosh and his co-researchers which portrays the significant genotoxic potential of cyclophosphamide [42]. In this regard, fisetin ruthenium-p-cymene complex treated animals demonstrated a significantly low incidence of chromosomal aberration as compared to the cyclophosphamide treated group. Thus, it can be stated that treatment with fisetin ruthenium-p-cymene complex does not have any genotoxic potential.

Fench and his colleagues reported that unedited chromosomal aberration in the M phase is primarily accountable for the development of micronucleus [43, 44]. The bone marrow micronucleus assay was carried out to further evaluate the genotoxic potential of the test compound. In this assay, the ratio of PCE (immature erythrocyte) to NCE (mature erythrocyte) was measured to assess the role of the complex on bone marrow differentiation. A downregulation of polychromatic erythrocytes (PCE) to normochromatic erythrocytes (NCE) ratio is a sign of bone marrow toxicity [45]. In our experiment we found that the cyclophosphamide treated group depicted a significant decrease in PCE/NCE with significant bone marrow suppression. Whereas, the complex treated groups showed no such alteration in the ratio of PCE/NCE as compared to the vehicle control group. Furthermore, we assessed the number of micronucleated polychromatic erythrocytes (MNPCE) which signifies the extra-nuclear bodies containing damaged chromosomal fragments [46]. The treatment with fisetin ruthenium-p-cymene complex significantly reduced the percentage of MNPCE (% of MN) but the cyclophosphamide treated group showed a significantly increased level of % MN in comparison to the vehicle control and complex treated groups. Taken together, the novel organometallic complex was not associated with any type of genetic mutation and chromosomal damage.

In conclusion, the safety profile of fisetin ruthenium-p-cymene complex was investigated and the LD_{50} value was found to be 500 mg/kg. Moreover, the safe dose of this novel organometallic complex was determined as 50, 100 and 200 mg/kg body weight which can be further investigated in our laboratory as a potential bioactive candidate to treat several ailments for optimum therapeutic intervention with further clinical assessment.

Acknowledgements The authors are grateful to the Department of Pharmacy, NSHM Knowledge Campus Kolkata-Group of Institution for their continuous support and encouragement throughout the experiment.

Author contributions All authors contributed to the study conception and design. Material preparation, data collection and analysis were performed by IS, SS, AD, and SR. The first draft of the manuscript was written by IS and all authors commented on previous versions of the manuscript. All authors read and approved the final manuscript.

Funding The authors declare that no funds, grants, or other support were received during the preparation of this manuscript.

Data availability The datasets are presented in the main manuscript.

Declarations

Conflict of interest The authors have no relevant financial or non-financial interests to disclose.

Ethical approval The animal experiment was approved by the Institutional Animal Ethics Committee and by the Animal Regulatory Body of the Government (Regd.No. 1458/PO/E/S/11/CPCSEA dated 12.05.2011).

References

1. Samanta A, Das G, Das SK (2011) Roles of flavonoids in plants. Int J Pharm Sci Technol 100:12–35
2. Feng W, Hao Z, Li M (2017) Isolation and structure identification of flavonoids. In: Flavonoids - from biosynthesis to human health. London, IntechOpen. https://doi.org/10.5772/67810
3. Rodríguez-García C, Sánchez-Quesada C, Gaforio JJ (2019) Dietary flavonoids as cancer chemopreventive agents: an updated review of human studies. Antioxidants 8:137. https://doi.org/10.3390/antiox8050137
4. Sun Y (1990) Free radicals, antioxidant enzymes, and carcinogenesis. Free Radic Biol Med 8:583–599. https://doi.org/10.1016/0891-5849(90)90156-d
5. Maher P, Akaishi T, Abe K (2006) Flavonoid fisetin promotes ERK-dependent long-term potentiation and enhances memory. Proc Natl Acad Sci U S A 103:16568–16573. https://doi.org/10.1073/pnas.0607822103
6. Khan N, Asim M, Afaq F, Abu Zaid M, Mukhtar H (2008) A novel dietary flavonoid fisetin inhibits androgen receptor signaling and tumor growth in athymic nude mice. Cancer Res 68:8555–8563. https://doi.org/10.1158/0008-5472.can-08-0240
7. Arai Y, Watanabe S, Kimira M, Shimoi K, Mochizuk R, Kinae N (2000) Dietary intakes of flavonols, flavones and isoflavones by Japanese women and the inverse correlation between quercetin intake and plasma LDL cholesterol concentration. J Nutr 130:2243–2250. https://doi.org/10.1093/jn/130.9.2243
8. Pal HC, Pearlman RL, Afaq F (2016) Fisetin and its role in chronic diseases. Adv Exp Med Biol 928:213–244. https://doi.org/10.1007/978-3-319-41334-1_10
9. Rengarajan T, Yaacob NS (2016) The flavonoid fisetin as an anticancer agent targeting the growth signaling pathways. Eur J Pharmacol 789:8–16. https://doi.org/10.1016/j.ejphar.2016.07.001
10. Ahmad S, Khan A, Ali W, Jo MH, Park J, Ikram M, Kim MO (2021) Fisetin rescues the mice brains against D-galactose-induced oxidative stress, neuroinflammation and memory impairment. Front Pharmacol 12:612078. https://doi.org/10.3389/fphar.2021.612078
11. Cordaro M, D'Amico R, Fusco R, Peritore AF, Genovese T, Interdonato L, Franco G, Arangia A, Gugliandolo E, Crupi R, Siracusa R, Di Paola R, Cuzzocrea S, Impellizzeri D (2022) Discovering the effects of fisetin on NF-κB/NLRP-3/NRF-2 molecular pathways in a mouse model of vascular dementia induced by repeated bilateral carotid occlusion. Biomed 10:1448. https://doi.org/10.3390/biomedicines10061448
12. Sun Y, Qin H, Zhang H, Feng X, Yang L, Hou DX, Chen J (2021) Fisetin inhibits inflammation and induces autophagy by mediating PI3K/AKT/mTOR signaling in LPS-induced RAW264.7 cells. Food Nutr Res. https://doi.org/10.29219/fnr.v65.6355
13. Kumar S, Pandey AK (2013) Phenolic content, reducing power and membrane protective activities of *Solanum xanthocarpum* root extracts. Vegetos–Int J Plant Res 26:301. https://doi.org/10.5958/j.2229-4473.26.1.043
14. Ikeda NEA, Novak EM, Maria DA, Velosa AS, Pereira RMS (2015) Synthesis, characterization and biological evaluation of rutin–zinc(II) flavonoid -metal complex. Chem Biol Interact 239:184–191. https://doi.org/10.1016/j.cbi.2015.06.011
15. Samsonowicz M, Regulska E, Kalinowska M (2017) Hydroxyflavone metal complexes - molecular structure, antioxidant activity and biological effects. Chem Biol Interact 273:245–256. https://doi.org/10.1016/j.cbi.2017.06.016
16. Zhang L, Liu Y, Wang Y, Xu M, Hu X (2018) UV–Vis spectroscopy combined with chemometric study on the interactions of three dietary flavonoids with copper ions. Food Chem 263:208–215. https://doi.org/10.1016/j.foodchem.2018.05.009
17. Dimitrić Marković JM, Marković ZS, Veselinović DS, Krstić JB, Predojević Simović JD (2009) Study on fisetin–aluminium(III) interaction in aqueous buffered solutions by spectroscopy and molecular modeling. J Inorg Biochem 103:723–730. https://doi.org/10.1016/j.jinorgbio.2009.01.005
18. Afanas'eva IB, Ostrakhovitch EA, Mikhal'chik EV, Ibragimova GA, Korkina LG (2001) Enhancement of antioxidant and anti-inflammatory activities of bioflavonoid rutin by complexation with transition metals. Biochem Pharmacol 61:677–684. https://doi.org/10.1016/s0006-2952(01)00526-3
19. Bors W, Heller W, Michel C, Saran M (1990) Flavonoids as antioxidants: determination of radical-scavenging efficiencies. Methods Enzymol 186:343–355. https://doi.org/10.1016/0076-6879(90)86128-i
20. Kostyuk V, Potapovich A, Vladykovskaya E, Korkina L, Afanas'ev I (2001) Influence of metal ions on flavonoid protection against asbestos-induced cell injury. Arch Biochem Biophys 385:129–137. https://doi.org/10.1006/abbi.2000.2118
21. Hartinger CG, Dyson PJ (2009) Bioorganometallic chemistry—from teaching paradigms to medicinal applications. Chem Soc Rev 38:391–401. https://doi.org/10.1039/b707077m
22. Raj Kumar R, Ramesh R, Małecki JG (2018) Synthesis and structure of arene ruthenium(II) benzhydrazone complexes: antiproliferative activity, apoptosis induction and cell cycle analysis. J Organomet Chem 862:95–104. https://doi.org/10.1016/j.jorganchem.2018.03.013
23. Bratsos I, Simonin C, Zangrando E, Gianferrara T, Bergamo A, Alessio E (2011) New half sandwich-type Ru(ii) coordination compounds characterized by the fac-Ru(dmso-S)3 fragment: influence of the face-capping group on the chemical behavior and in vitro anticancer activity. Dalton Trans 40:9533. https://doi.org/10.1039/c1dt11043h
24. Jamieson ER, Lippard SJ (1999) Structure, recognition, and processing of cisplatin−DNA adducts. Chem Rev 99:2467–2498. https://doi.org/10.1021/cr980421n
25. Chu G (1994) Cellular responses to cisplatin. The roles of DNA-binding proteins and DNA repair. J Biol Chem 269:787–790. https://doi.org/10.1016/s0021-9258(17)42175-2
26. Galanski M (2006) Recent developments in the field of anticancer platinum complexes. Recent Pat Anticancer Drug Discov 1:285–295. https://doi.org/10.2174/157489206777442287
27. Samimi G, Kishimoto S, Manorek G, Breaux JK, Howell SB (2006) Novel mechanisms of platinum drug resistance identified in cells selected for resistance to JM118 the active metabolite of satraplatin. Cancer Chemother Pharmacol 59:301–312. https://doi.org/10.1007/s00280-006-0271-0
28. Huang H, Zhang P, Yu B, Chen Y, Wang J, Ji L, Chao H (2014) Targeting nucleus DNA with a cyclometalated dipyridophenazineruthenium(II) complex. J Med Chem 57:8971–8983. https://doi.org/10.1021/jm501095r
29. Rahman MM, Islam MB, Biswas M, Khurshid Alam AH (2015) In vitro antioxidant and free radical scavenging activity of different parts of Tabebuia pallida growing in Bangladesh. BMC Res Notes 8:621. https://doi.org/10.1186/s13104-015-1618-6
30. Benzie IF, Strain JJ (1996) The ferric reducing ability of plasma (FRAP) as a measure of "antioxidant power": the FRAP assay. Anal Biochem 239:70–76. https://doi.org/10.1006/abio.1996.0292

31. Griffin SP, Bhagooli R (2004) Measuring antioxidant potential in corals using the FRAP assay. J Exp Mar Biol Ecol 302:201–211. https://doi.org/10.1016/j.jembe.2003.10.008
32. Pennycooke JC, Cox SE, Stushnoff C (2005) Relationship of cold acclimation, total phenolic content and antioxidant capacity with chilling tolerance in petunia (Petunia hybrid). Environ Exp Bot 53:225–232. https://doi.org/10.1016/j.envexpbot.2004.04.002
33. Maron DM, Ames BN (1983) Revised methods for the Salmonella mutagenicity test. Mutat Res 113:173–215. https://doi.org/10.1016/0165-1161(83)90010-9
34. Llana-Ruiz-Cabello M, Maisanaba S, Puerto M, Prieto AI, Pichardo S, Moyano R, González-Pérez JA, Cameán AM (2016) Genotoxicity evaluation of carvacrol in rats using a combined micronucleus and comet assay. Food Chem Toxicol 98:240–250. https://doi.org/10.1016/j.fct.2016.11.005
35. Murakami M, Hirano T (2008) Intracellular zinc homeostasis and zinc signaling. Cancer Sci 99:1515–1522. https://doi.org/10.1111/j.1349-7006.2008.00854.x
36. Sliwinski T, Czechowska A, Kolodziejczak M, Jajte J, Wisniewska-Jarosinska M, Blasiak J (2009) Zinc salts differentially modulate DNA damage in normal and cancer cells. Cell Biol Int 33:542–547. https://doi.org/10.1016/j.cellbi.2009.02.004
37. Costello LC, Franklin RB (2012) Cytotoxic/tumor suppressor role of zinc for the treatment of cancer: an enigma and an opportunity. Expert Rev Anticancer Ther 12:121–128. https://doi.org/10.1586/era.11.190
38. Soto AM, Sonnenschein C (2004) The somatic mutation theory of cancer: growing problems with the paradigm? Bioassays 26:1097–1107. https://doi.org/10.1002/bies.20087
39. Mortelmans K, Zeiger E (2000) The Ames Salmonella/microsome mutagenicity assay. Mutat Res 455:29–60. https://doi.org/10.1016/s0027-5107(00)00064-6
40. Phillips DH, Arlt VM (2009) Genotoxicity: damage to DNA and its consequences. EXS 99:87–110. https://doi.org/10.1007/978-3-7643-8336-7_4
41. Genetic Alliance, The New York-Mid-Atlantic Consortium for Genetic and Newborn Screening Services (2009) Understanding genetics: a New York, Mid-Atlantic guide for patients and health professionals. Genetic alliance.
42. Ghosh N, Sandur R, Ghosh D, Roy S, Janadri S (2017) Acute, 28days sub acute and genotoxic profiling of quercetin-magnesium complex in Swiss albino mice. Biomed Pharmacother 86:279–291. https://doi.org/10.1016/j.biopha.2016.12.015
43. Fenech M, Kirsch-Volders M, Natarajan AT, Surralles J, Crott JW, Parry J, Norppa H, Eastmond DA, Tucker JD, Thomas P (2010) Molecular mechanisms of micronucleus, nucleoplasmic bridge and nuclear bud formation in mammalian and human cells. Mutagenesis 26:125–132. https://doi.org/10.1093/mutage/geq052
44. Ikken Y, Morales P, Martínez A, Marín ML, Haza AI, Cambero MI (1999) Antimutagenic effect of fruit and vegetable ethanolic extracts against N-nitrosamines evaluated by the Ames test. J Agric Food Chem 47:3257–3264. https://doi.org/10.1021/jf990166n
45. Suzuki Y, Nagae Y, Li J, Sakaba H, Mozawa K, Takahashi A, Shimizu H (1989) The micronucleus test and erythropoiesis. Effects of erythropoietin and a mutagen on the ratio of polychromatic to normochromatic erythrocytes (P/N ratio). Mutagenesis 4:420–424. https://doi.org/10.1093/mutage/4.6.420
46. Luzhna L, Kathiria P, Kovalchuk O (2013) Micronuclei in genotoxicity assessment: from genetics to epigenetics and beyond. Front Genet 4:131. https://doi.org/10.3389/fgene.2013.00131